JAST, Vol. 3, No. 4, pp 185–193
© Iranian Aerospace Society, December 2006

JAST
Journal of Aerospace Science and Technology

Mixed-mode I/II Interlaminar Fracture of CF/PEI Composite Material

N. Choupani[1]

Failures in composite materials occur mainly due to interlaminar fracture, also called delamination, between laminates. This indicates that characterizing interlaminar fracture toughness is the most effective factor in the fracture of composite materials. This study reports investigation on mixed-mode interlaminar fracture behaviour in woven carbon fibre/polyetherimide (CF/PEI) thermoplastic composite material based on experimental and numerical analyses. Experiments were conducted using the special test loading device. By varying the loading angle,α from 0^o to 90^o, pure mode-I, pure mode-II and a wide range of mixed-mode data were obtained experimentally. Using the finite-element results, geometrical factors were applied to the specimen. Based on experimentally measured critical loads, mixed-mode interlaminar fracture toughness for the composite under consideration determined. The fracture surfaces were examined by scanning electron microscopy to gain insight into the failure responses.

INTRODUCTION

Various applications of composite materials in primary and secondary load-bearing structures have established them as a good substitute for metallic materials. Composite materials with the great advantage of strength and stiffness combined with lightness have proved their usefulness through many applications in various fields, in particular in aerospace applications. Due to their importance in engineering applications a great effort has been spent in the study of the failure behaviour of composite materials and structures [1-10]. Failures in composite materials occur mainly due to interlaminar fracture, also called delamination, between laminates. This indicates that characterizing interlaminar fracture toughness is one of the most effective factor in determining the fracture of composite materials.

In recent years, many test methods have been proposed by many researchers to determine interlaminar fracture toughness for three modes of loading (I, II, and III) and also under mixed-mode conditions [4, 7-23]. The double cantilever beam (DCB) test is the most widely used method for measuring mode-I (opening) interlaminar fracture toughness. The end-notched flexure (ENF) has emerged as one of the most convenient mode-II (sliding shear) interlaminar fracture specimens. A crack rail shear (CRS) specimen has been proposed to determine the mode-III (tearing) critical strain energy release rate. However, due to the strong anisotropy of composite structures, the fracture is usually not a result of pure mode-I or pure mode-II loading, and the delamination occurs in the mixed-mode loading conditions. For this reason, the study of the mixed-mode interlaminar fracture toughness is very important.

Various attempts have been made to characterize interlaminar fracture toughness under mixed-mode loading conditions, but mostly beam type specimens have been used [12-14, 24-30]. Some of these include: the mixed-mode flexure (MMF) test, the end loaded split (ELS) specimen, the single leg bending (SLB) specimen, the crack lap shear (CLS) test, the edge delamination tension (EDT) specimen, and the asymmetric double cantilever beam. However, for all these test methods there are problems in that a wide range of mixed-mode ratios cannot be tested which limits their usefulness. The mixed-mode bending (MMB) test has been proposed by combining the schemes used for DCB and ENF tests, which can produce a wide range of the ratios of mode-I and mode-II components by varying the lever arm of the specimen [12-14, 22, 24, 25, 31, 32]. But in order to obtain reliable results for

1. *Assistant Professor, Dept. of Mech. Eng., Sahand Univ. of Tech., Tabriz, Iran, E-mail: Choupani@sut.ac.ir.*

interlaminar fracture toughness for pure mode-I, pure mode-II, and mixed-mode loading conditions, different beam type specimens would be required. It is therefore necessary to develop other test methods to evaluate the interlaminar fracture parameters of composite materials under all in-plane loading conditions starting from pure mode-I to pure mode-II.

In this study, a modified version of the Arcan specimen was made for the mixed-mode fracture test of CF/PEI specimens, which allows mode-I, mode-II, and almost any combination of mode-I and mode-II loading to be tested with the same test specimen configuration [33-35]. Therefore, disadvantages presented in the previous mixed-mode toughness test methods can be avoided. This investigation seeks to extend understanding of the interlaminar fracture behaviour of a woven carbon fibre/polyetherimide (CF/PEI) thermoplastic composite material under mixed-mode loading conditions through numerical and experimental methods.

INTERLAMINAR FRACTURE

The determination of resistance to delamination is very important, since composite materials have superior properties only in the fibre direction. Resistance to delamination is known as the interlaminar fracture toughness or interlaminar fracture resistance. There are extensive research activities in the field of interlaminar fracture of composite materials theoretically, experimentally and numerically [5, 9, 10, 26, 27, 36, 37]. Linear elastic fracture mechanics has been found useful tool for the field of interlaminar cracks in composites. For many composites crack growth is self-similar because of delamination and this leads to partition G value into modes-I and II [5]. The energy release rates for orthotropic material with the crack line parallel to the principal orthotropic direction which coincides with the fiber orientation, can be calculated from the following relationships [2-4, 6, 38]:

$$G_I = K_I^2/E_I, \quad G_{II} = K_{II}^2/E_{II} \tag{1}$$

where E_I and E_{II} are effective moduli, and K_I and K_{II} are mode-I and mode-II stress intensity factors, respectively. It is assumed that the specimens are orthotropic linear elastic material and effective moduli E_I and E_{II} for plane strain conditions are defined as:

$$E_I = \sqrt{\frac{2}{b_{11}b_{22}}} \cdot \frac{1}{\sqrt{\sqrt{\frac{b_{22}}{b_{11}}} + \frac{2b_{12}+b_{66}}{2b_{11}}}},$$

$$E_{II} = \frac{\sqrt{2}}{b_{11}} \cdot \frac{1}{\sqrt{\sqrt{\frac{b_{22}}{b_{11}}} + \frac{2b_{12}+b_{66}}{2b_{11}}}} \tag{2}$$

where the terms of the constants b_{ij} are defined in terms of the following nonzero entries a_{ij} of the orthotropic compliance matrix:

$$b_{ij} = a_{ij} - \frac{a_{i3}a_{j3}}{a_{33}} \; (i,j = 1,2,4,5,6)$$

and the terms of the nonzero entries a_{ij} of the orthotropic compliance matrix are defined in terms of the following engineering elastic constants [4, 6, 36, 38]:

$$a_{11} = \frac{1}{E_x}, \quad a_{22} = \frac{1}{E_y}, \quad a_{33} = \frac{1}{E_z},$$

$$a_{44} = \frac{1}{G_{yz}}, \quad a_{55} = \frac{1}{G_{xz}}, \quad a_{66} = \frac{1}{G_{xy}},$$

$$a_{12} = a_{21} = -\frac{\nu_{xy}}{E_x} = -\frac{\nu_{yx}}{E_y},$$

$$a_{13} = a_{31} = -\frac{\nu_{xz}}{E_x} = -\frac{\nu_{zx}}{E_z},$$

$$a_{23} = a_{32} = -\frac{\nu_{yz}}{E_y} = -\frac{\nu_{zy}}{E_z} \tag{3}$$

The stress intensity factors ahead of the crack tip for a modified version of Arcan specimen were

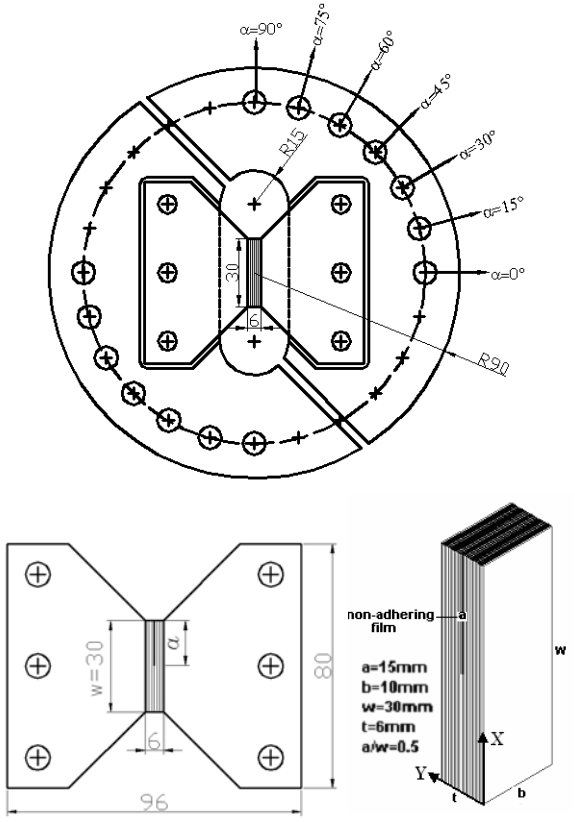

Figure 1. Geometry of the loading and modified version of Arcan specimen, dimensions are given in mm.

calculated by using the following equations [33-35, 39-44]:

$$K_I = \frac{P_c\sqrt{\pi a}}{wt} f_1(a/w)$$

$$K_{II} = \frac{P_c\sqrt{\pi a}}{wt} f_2(a/w) \quad (4)$$

where P_c is critical load at fracture, w is specimen length, t is specimen thickness and a is crack length. In turn K_I and K_{II} are obtained using geometrical factors $f_1(a/w)$ and $f_2(a/w)$, respectively, which are obtained through finite element analysis of Arcan test specimen.

EXPERIMENTAL PROCEDURES

Materials and Specimens

A modified version of the Arcan test apparatus was used to measure the mixed-mode interlaminar fracture toughness of carbon fibre/polyetherimide (CF/PEI) thermoplastic composite material. High strain to failure, increased fracture toughness, better impact tolerance, short processing cycle time, unlimited shelf life of prepreg, recyclability, repairability, cost effective processing, excellent toughness and damage tolerance are some of the advantages for CF/PEI composite material [45, 46]. In the experiment, a woven plate consisting of 22 plies of CF/PEI prepergs, in order to obtain a plate thickness of approximately 6mm were used. During the lay up of prepergs by hand to the required number of plies, a UPLEX®-R-25 film (25 μm in thickness) was placed between the central plies in order to introduce a starter crack.

The composite plates were produced using a hot press. Curing of CF/PEI composite was performed using the following procedures: cover tool with UPLEX®-R-50 film (50 μm in thickness), place desired lay-up of prepregs (22 plies) on covered tool, preheat at 320 °C for 25 minutes under an applied pressure of 2.5 MPa using a hot press, cool the mould under pressure to a temperature far below the glass transition temperature of 217 °C. The specimens were cut with a diamond wheel and machined to the dimensions of 30x10x6 mm. The elastic constants of plate used in FEM analyses are summarized in Table 1 [47]. For CF/PEI composite material, 1 is the direction parallel to the crack and 2 and 3 are the directions transverse to the crack, while the direction of the crack coincides with the fibre direction (Figure 1).

Test Method and Setup

The composite strip was attached into aluminum plates using FM®300-2 adhesive. Bonding was carried out using a special jig to ensure alignment of the specimen halves. FM®300-2 is a high strength rubber modified film adhesive widely used for bonding composite structures in aerospace bonding applications. The adhesive was processed according to the manufacturer's specification [47, 48].

Table 1. Elastic Properties of CF/PEI composite [GPa].

E_1	E_2	E_3	G_{12}	G_{13}	G_{23}	ν_{12}	ν_{13}	ν_{23}
57.6	57.6	8.7	3.1	2.8	2.8	0.03	0.4	0.4

Figure 2. Overview of loading device and test set up: (a) Pure mode-I test; (b) Mixed-mode test; (c) Pure mode-II test.

For surface preparation of aluminum plates, FPL-Etch method was applied [49]. Composite surface preparation method involved degreasing with methyl ethyl ketone (MEK), rinse and check for water break, hand abrasion with 320 grit aluminum oxide abrasive papers and clean for bonding [50]. The specimens were pinned into the loading device in order to transmit the applied loads. The loading device and modified version of Arcan specimen are shown in Figure 2. This specimen was used in order to study the mixed-mode interlaminar fracture toughness of a CF/PEI composite material. With the application of load P and by varying the loading angle,α from 0^o to 90^o , pure mode-I, pure mode-II, and all mixed-mode loading conditions can be created and tested. Fracture tests were conducted by controlling the constant displacement rate of 0.2 mm/min and the fracture loads and displacements were recorded. All tests were carried out using an Instron 5567 testing machine. Tests were repeated 3 times for every loading angle.

FINITE ELEMENT ANALYSIS

The method used to calculate the stress intensity factor was an interaction J-integral method performed in

ABAQUS, and is required to separate the components of the stress intensity factors for a crack under mixed-mode loading in conjunction of finite element analysis. The method is applicable to cracks in isotropic and anisotropic materials. Based on the definition of the J-integral, the interaction integrals can be directly related to the stress intensity factors as [52]:

$$\mathbf{K} = 4\pi \mathbf{B} \cdot \mathbf{J}_{\text{int}} \tag{5}$$

where $\mathbf{B}$ is called the pre-logarithmic energy factor matrix, $\mathbf{K} = [K_I, K_{II}, K_{III}]^T$ and $\mathbf{J_{int}} = \left[J_{int}^I, J_{int}^{II}, J_{int}^{III}\right]^T$.

In linear elastic fracture mechanics, the J integral coincides with total energy release rate, $J = G_T = G_I + G_{II} + G_{III}$,where G_I, G_2 and G_{III} are the energy release rates associated with the mode-I, mode-II and mode-III stress intensity factors. Numerical analyses were carried out using the interaction J-integral method. Figure 3 shows example of the mesh pattern of the specimen, which were performed with ABAQUS under a constant load of 1000 N. The entire specimen was modeled using eight node collapsed quadrilateral element and the mesh was refined around crack tip, so that the smallest element size found in the crack tip elements was approximately 0.25 mm. A linear elastic finite element analysis was performed under a plane strain condition using $1/r^{0.5}$ stress field singularity. To obtain a $1/r^{0.5}$ singularity term of the crack tip stress field, the elements around the crack tip were focused on the crack tip and the mid side nodes were moved to a quarter point of each element side.

RESULTS AND DISCUSSION

In order to assess geometrical factors or non-dimensional stress intensity factors $f_I\,(a/w)$ and $f_{II}\,(a/w)$ for CF/PEI composite, the a/w ratio was varied between 0.3 and 0.7 at 0.1 intervals and a fourth order polynomial was fitted through finite element

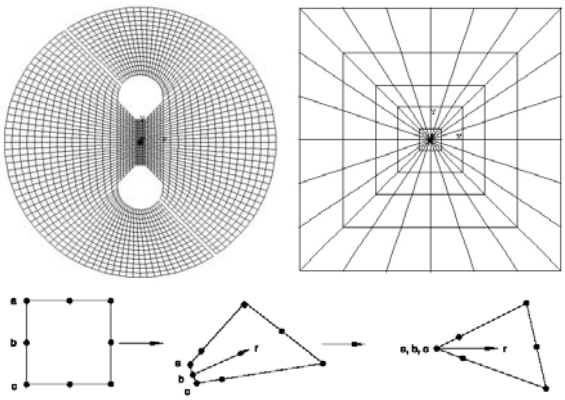

Figure 3. Finite element mesh pattern of the entire specimen and around the crack-tip of CF/PEI composite with crack length a= 15 mm.

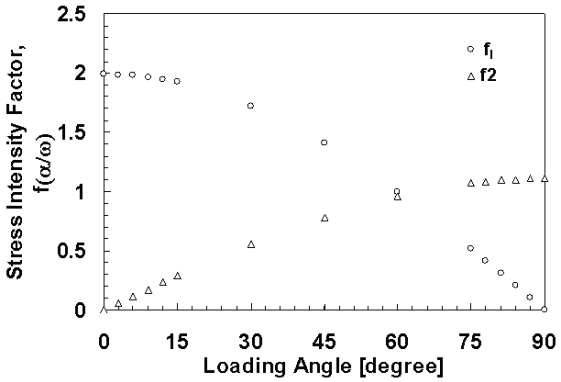

Figure 4. Non-dimensional stress intensity factors vs. loading angle of CF/PEI composite for the crack length a= 15 mm.

analysis as:

$$f_I(a/w)(\alpha = 0^\circ) = 182.12\,(a/w)^4 - 293.81\,(a/w)^3 + 187.87\,(a/w)^2 - 51.492\,(a/w) + 6.1137$$

and

$$f_{II}(a/w)(\alpha = 90^\circ) = -18.622\,(a/w)^4 + 36.753\,(a/w)^3 - 25.182\,(a/w)^2 + 7.759\,(a/w) + 0.0944 \tag{6}$$

Here a/w is the crack length ratio, where a is the rack length and w is the specimen length.

The relationship between the non-dimensional stress intensity factor and the loading angle is shown in Figure 4. It can be seen that for loading angles $\alpha \leq 60^o$, the mode-I fracture is dominant and as the mode-II loading contribution increases, the mode-I stress intensity factor decreases and the mode-II stress intensity factor increases. For $\alpha \geq 75^o$ mode-II fracture becomes dominant.

The strain energy release rates were calculated using Equations 1. The relationship between the mixed-mode ratios of strain energy release rates and the loading angles α is shown in Figure 5. For loading angles close to pure mode-I loading, very high ratios of mode-I to mode-II are dominant. The ratios of strain energy release rates close to pure mode-II loading exhibit the opposite trend.

As expected, it is confirmed that by varying the loading angle of the Arcan specimen, pure mode-I, pure mode-II and a wide range of mixed-mode loading conditions can be created and tested.

Table 2. Average critical mixed-mode interlaminar fracture loads P_C [N] for CF/PEI composite with crack length 15 mm.

Loading Angle		0	15	30	45	60	75	90
P_C	1	2023	2137	2216	2640	3490	4936	6776
	2	1813	1851	2102	2606	3201	4895	6285
	3	1702	1746	1884	2320	3114	4369	6282
	Avg.	1846	1911	2067	2522	3269	4734	6448

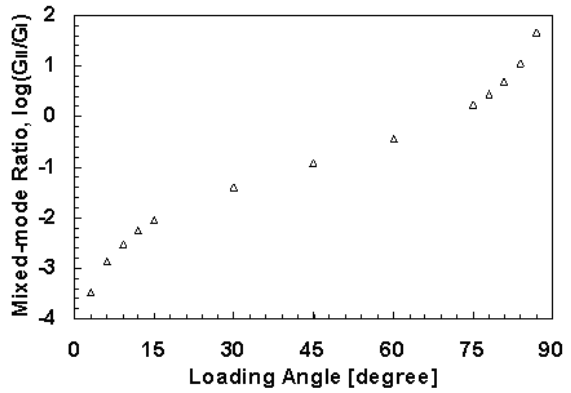

Figure 5. The ratio of mode-II to mode-I, G_{II}/G_I (in logarithmic scale), versus loading angle,α for CF/PEI composite with crack length a= 15 mm.

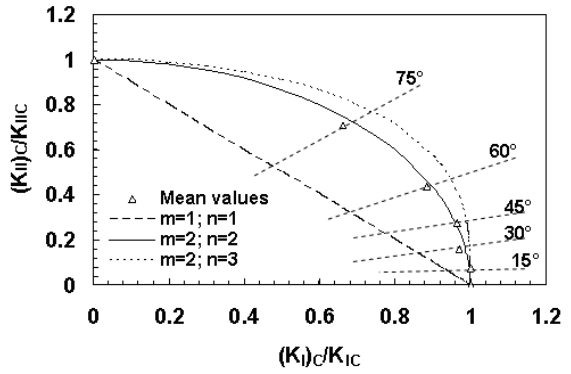

Figure 6. Predictions of the mixed-mode interlaminar fracture criteria of CF/PEI composite with crack length 15 mm.

Pure mode-I, pure-mode-II and five mixed-mode loading conditions were used as shown in Table 2. Tests were repeated at least 3 times for each loading angle and a total of 21 specimens were tested in this survey. The load-displacement curves generated by the test machine were used to determine maximum load and displacement. The average values of critical fracture loads were used to determine the critical mixed-mode stress intensity factors and strain energy release rates data. The fracture was found to be brittle with the load-deflection curves showing very little non-linearity.

The interlaminar fracture toughness was determined experimentally with the modified version of the Arcan specimen under different mixed-mode loading conditions. The calculated critical interlaminar strain energy release rate values $(G_I)_C$ and $(G_{II})_C$ using experimental data under various loading conditions are summarized in Table 3. $(G_I)_C$ decreases while $(G_{II})_C$ increases with an increase in mode-II loading contribution. The opening-mode and shearing-mode interlaminar critical strain energy release rates were found approximately 788 J/m^2 and 1160 J/m^2, respectively. It can be seen that G_{IIC} is larger than G_{IC}, indicating that the interlaminar cracked specimen is tougher in mode-II and weaker in mode-I loading conditions. Table 3 also shows the total interlaminar strain energy release rate, $(G_T)_C$= $(G_I)_C$+$(G_{II})_C$ under various loading conditions, which increases with the loading angle. Therefore, it is confirmed that the maximum fracture toughness occurs at mode-II loading condition. Several studies have been conducted to obtain a suitable description of mixed-mode fracture behaviour in composites [12-14, 24, 26, 27, 33, 35]. It is generally proposed in the form of:

$$\left(\frac{(K_I)_C}{K_{IC}}\right)^m + \left(\frac{(K_{II})_C}{K_{IIC}}\right)^n = 1 \qquad (7)$$

Jurf and Pipes [33] reported that the quadratic form of m=2 and n=2 is suitable for mixed-mode fracture criteria of ASI/3501-6 graphite/epoxy composite material. Yoon and Hong [35] found that a relation of the form m=2 and n=3 provided a better fitting of the experimental data. The interlaminar fracture toughness was determined experimentally with the modified version of the Arcan specimen for CF/PEI composite under different mixed-mode loading conditions. A failure criterion was developed by plotting the average fracture toughness data on a non-dimensional diagram (Figure 6). It can be seen that an elliptical equation (m=2 and n=2) is suitable for characterizing the mixed-mode fracture criterion of interlaminar fracture of CF/PEI composite, as the experimental results are below the elliptic failure assessment curve.

Scanning electron microscopy (SEM) of fracture surfaces of the mode-I specimens are shown in Figures 7 and 8. Figure 7 shows the fractograph of the mode-I fracture of the initiation area taken just beyond the precrack insert film of the CF/PEI composite. Therefore, the fracture surfaces show the first increment of interlaminar crack growth which corresponds to the measured fracture toughness. The mode-I fracture surface is indicative of a brittle cleavage failure with relatively smooth and flat matrix fracture and shows debonding between fibre and matrix, which would explain the low mode-I fracture toughness. Figure 8 shows the fractograph of a mode-I fracture of the propagation area. Its characteristic is overall flatness on the matrix fracture. Figures 9 and 10 show the interlaminar fracture surfaces at mixed-mode loading conditions (α = 45°) for the CF/PEI composite. As discussed earlier, at pure mode-É the fracture surface was very flat indicating a brittle cleavage fracture which

Table 3. Average Interlaminar critical strain energy release rates G_C [J/m^2] for CF/PEI composite with crack length 15 mm.

Loading Angle	0	15	30	45	60	75	90
$(G_I)_C$	787.8	788.1	741.0	735.0	616.9	345.8	-
$(G_{II})_C$	-	6.8	29.8	88.7	223.5	583.1	1159.8
$(G_T)_C$	787.8	794.9	770.8	823.7	840.4	928.9	1159.8

would explain the low mode-I fracture toughness. As mode-II loading contribution is added, the fracture surfaces become rougher as seen in the micrograph taken just after the precrack insert film for the CF/PEI composite under mixed-mode ($\alpha = 45°$) loading conditions (Figure 9). Troughs and hackles have appeared where fibres have been pulled away from the matrix indicating interfacial failure (Figure 10). Hackles are regions of the matrix deformation between adjacent fibres that are lifted up parallel to one another and tend to slant in the same direction over the entire surface.

SEM of fracture surfaces of the mode-II specimens are shown in Figures 11 and 12. A scanning electron micrograph of the area at the rear of the crack tip of the fracture surface of the Mode-II specimen is shown in Figure 11. Everywhere on the fracture surface of the specimens, broken fibres were observed, as the marks of fibre-matrix debonding and hackles accompanied by fragmentation of the matrix phase. Figure 12 shows the fractograph of a mode-II fracture at the propagation area. Its characteristic is numerous inclined hackles of the matrix fracture and troughs where fibres have been pulled away from the matrix indicating interfacial failure.

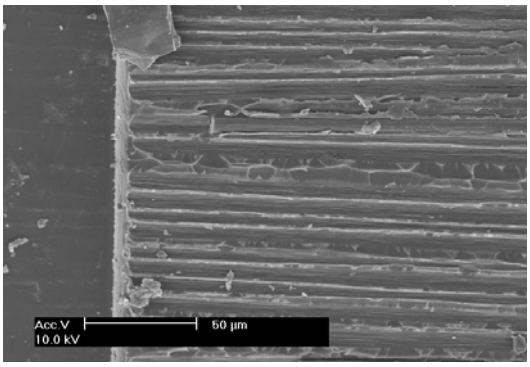

Figure 7. SEM micrograph of a mode-I ($\alpha = 0°$) fracture surface of CF/PEI composite: initiation areas. The arrow indicates the direction of crack propagation.

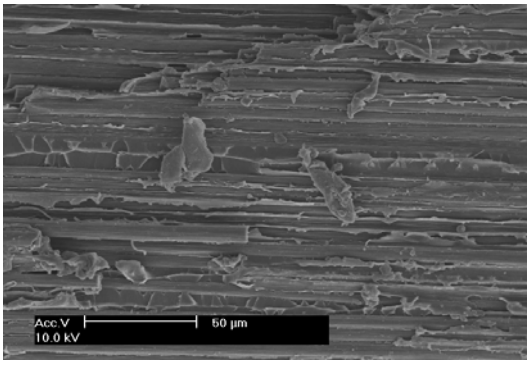

Figure 8. SEM micrograph of a mode-I ($\alpha = 0°$) fracture surface of CF/PEI composite: propagation areas. The arrow indicates the direction of crack propagation.

CONCLUSION

In this paper the mixed-mode interlaminar fracture behaviour for CF/PEI composite specimens was investigated based on experimental and numerical analyses. A modified version of Arcan specimen was employed to conduct mixed-mode test using the special test loading device. The full range of mixed-mode loading conditions including pure mode-I and pure mode-II loading can be created and tested. It is a simple test procedure, clamping/unclamping the specimens is easy to achieve and only one type of specimen is required to generate all loading conditions.

The finite element results indicate that for loading angles close to pure mode-II loading, a high ratio of mode-II to mode-I fracture is dominant and there is an opposite trend for loading angles close to pure mode-I loading. It confirms that by varying the loading angle of Arcan specimen pure mode-I, pure mode-II and a wide range of mixed-mode loading conditions can be created and tested. Also, numerical results confirm that the increase of the mode-II loading contribution leads to an increase of fracture resistance in the CF/PEI composite (i.e., a reduction in the total strain energy release rate) and the increase of the crack length

Figure 9. SEM micrograph of a mixed-mode ($\alpha = 45°$) fracture surface of CF/PEI composite: initiation areas. The arrow indicates the direction of crack propagation.

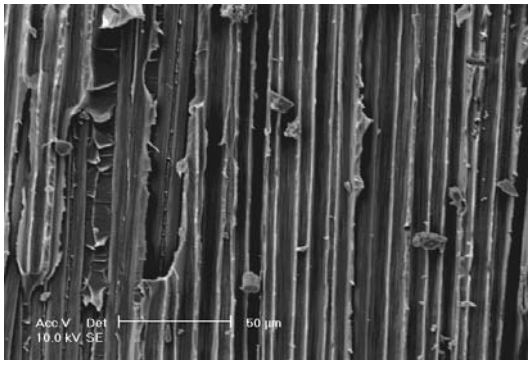

Figure 10. SEM micrograph of a mixed-mode ($\alpha = 45°$) fracture surface of CF/PEI composite: propagation areas. The arrow indicates the direction of crack propagation.

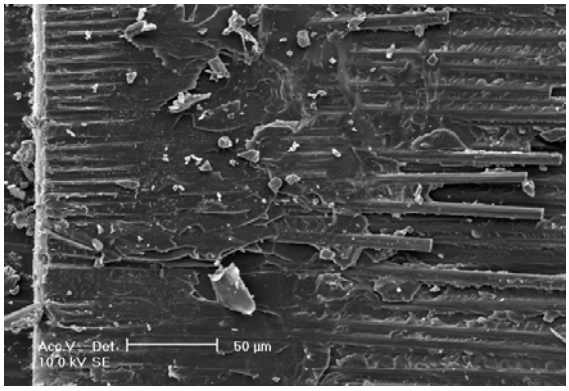

Figure 11. SEM micrograph of a mode-II ($\alpha = 90^\circ$) fracture surface of CF/PEI composite: initiation areas. The arrow indicates the direction of crack propagation.

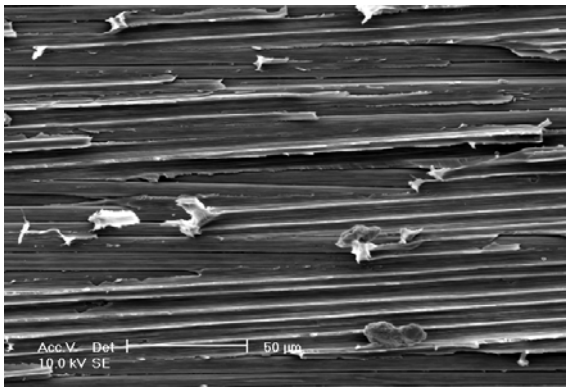

Figure 12. SEM micrograph of a mode-II ($\alpha = 90^\circ$) fracture surface of CF/PEI composite: propagation areas. The arrow indicates the direction of crack propagation.

leads to a reduction of interlaminar fracture resistance in the CF/PEI composite (i.e., an increase in the total interlaminar strain energy release rate).

The interlaminar fracture toughness was determined experimentally with the modified version of the Arcan specimen under different mixed-mode loading conditions. The results indicated that the interlaminar cracked specimen is tougher in shear loading conditions and weaker in tensile loading condition and an elliptical equation (m=2 and n=2) was found to be suitable for characterizing the mixed-mode fracture criterion of the interlaminar fracture of the CF/PEI composite. The SEM fracture surfaces observations showed that the mode-I fracture surface was indicative of a brittle cleavage failure with relatively smooth and flat matrix fracture and showed only little debonding between fibre and matrix. As the mode-II loading contribution was added, the fracture surfaces became rougher and troughs and hackles appeared. Everywhere on the mode-II fracture surface of the specimens, broken fibres, troughs and hackles were observed.

ACKNOWLEDGMENTS

I owe special thanks to professor Lin Ye and his research group for their valuable time, advice, guidance, and support throughout my study. The School of Aerospace, Mechanical and Mechatronic Engineering and the Electron Microscope Unit at the University of Sydney has kindly provided access to their facilities.

REFERENCES

1. Buchholz, F.G., Rikards R., and Wang H., "Computational Analysis of Interlaminar Fracture of Laminated Composites", *International Journal of Fracture*, **86**, PP 37-57(1997).
2. Sih, G.C., *Engineering Application of Fracture Mechanics*, Kluwer Academic, PP 279-305.
3. Gibson, R.F., *Principles of Composite Material Mechanics*, Mcgraw-Hill, (1994).
4. Gillespie, J.W. and Carlsson L.A., *Delaware Composites Design Encyclopedia*, Technomic, PP 113-119(1990).
5. Williams, J.G., "Application of Fracture Mechanics to Comosite Materials", PP 3-39(1989).
6. Sih, G.C. and Chen E.P., "Cracks in Composite Materials: A Compilation of Stress Solutions for Composite Systems with Cracks", *Mechanics of Fracture*, **6**, PP 538(1981).
7. Stevanovic, D., Kalyanasundaram S., Lowe A. and Jar P.-Y.B., "Mode I and Mode II Delamination Properties of Glass/Vinyl-Ester Composite Toughened by Particulate Modified Interlayers", *Composites Science and Technology*, **63**(3), PP 1949-1964(2000).
8. O'Brien, T.K., "Interlaminar Fracture Toughness: The Long and Winding Road to Standardization", *Composites Part B: Engineering*, **29**(1), PP 57-62(1998).
9. Davidson, B.D., "A Predictive Methodology for Delamination Growth in Laminated Composites, Part I: Theoretical Development and Preliminry Experimental Results", Syracuse University, Washington, PP 50(1998).
10. Davidson, B.D., "A Predictive Methodology for Delamination Growth in Laminated Composites Part I: Analysis, Applications, and Accuracy Assessment", Syracuse University, Washington, PP 126(2001).
11. Miyagawa, H., Sato C. and Ikegami K., "Fracture Toughness Evaluation for Multidirectional Cfrp by the Raman Coating Method", *Composites Science and Technology*, **60**, PP 2903-2915(2000).
12. Ducept, F., Davies P. and Gamby D., "Mixed Mode Failure Criteria for a Glass/Epoxy Composite and an Adhesively Bonded Composite/Composite Joint", *International Journal of Adhesion & Adhesives*, 233-244, **20**, (2000).
13. Ducept, F., Davies P. and Gamby D., "An Experimental Study to Validate Tests Used to Determine Mixed Mode Failure Criteria of Glass/Epoxy Composites", *Composites Part A: Applied Science and Manufacturing*, **28**(8), PP 719-729(1997).

14. Ducept, F., Gamby D. and Davies P., "A Mixed-Mode Failure Criterion Derived from Tests on Symmetric and Asymmetric Specimens", *Composites Science and Technology*, **59**(4), PP 609-619(1999).
15. Warrior, N.A., Pickett A.K. and Lourenco N.S.F, "Mixed-Mode Delamination - Experimental and Numerical Studies", *Strain*, **39**(4), PP 153-159(2003).
16. Kikuchi, M. and Kuroda M., "Mixed-Mode Fracture Test of Cfrp Laminates", *JSME International Journal*, **35**(4), PP 496-501(1992).
17. Fox, B.L., "The Manufacturing Charaterization and Aging of Novel High Temperature Carbon Fibre Composites", Ph.D. Thesis, The Australian National University(2001).
18. Naik, N.K., Reddy K.S., Meduri S., Raju N.B., Prasad P.D., Azad S.N.M., Ogde P.A and Reddy B.C.K, "Interlaminar Fracture Characterization for Plain Weave Fabric Composites", *Journal of Materials Science*, **37**(14), PP 2983-2987(2002).
19. Hansen, P. and Martin R., "DCB, 4ENF and MMB Delamination Characterisation of S2 8552", Materials Engineering Research Laboratory LTD. Hertford, England, PP 42(1999).
20. O'BRIEN, T.K., "Interlaminar Fracture of Composites", NASA Langley Research Center, Hampton: Washington, PP 40(1984).
21. Funk, J.G. and Deaton J.W., "Interlaminar Fracture Toughness of Woven Graphite/Epoxy Composites", NASA Langley Research Center: Hampton, PP 29(1989).
22. Benzeggagh, M.L. and Kenane M., "Measurement of Mixed-Mode Delamination Fracture Toughness of Unidirectional Glass/Epoxy Composites with Mixed-Mode Bending Apparatus", *Composites Science and Technology*, **56**(4), PP 439-449(1996).
23. Hashemi, S., Kinloch A.J. and Williams J.G., "Mechanics and Mechanisms of Delamination in a Poly(Ether Sulphone)-Fibre Composite", *Composites Science and Technology*, **37**, PP 429-462(1990).
24. Reeder, J.R., "An Evaluation of Mixed-Mode Delamination Failure Criteria", *NASA TECHNICAL MEMORANDUM 104210*, National Aeronautics and Space Administration Langley Research Center Hampton, Virginia, PP 1-34(1992).
25. Reeder, J.R. and Crews J.R., "Mixed-Mode Bending Method for Delamination Testing", *AIAA Journal*, **28**(7), PP 1270-1276(1990).
26. Rikards, R., Buchholz F.-G., Wang H., Bledzki A.K., Korjakin A. and Richard H.-A., "Investigation of Mixed Mode I/Ii Interlaminar Fracture Toughness of Laminated Composites by Using a Cts Type Specimen", *Engineering Fracture Mechanics*, **61**(3-4), PP 325-342(1998).
27. Rikards, R., "Interlaminar Fracture Behaviour of Laminated Composites", *Computers & Structures*, **76**(1-3), PP 11-18(2000).
28. Crews, J.H. and Reeder J.R., "A Mixed-Mode Bending Apparatus for Delamination Testing", National Aeronautics and Space Administration, Viriginia, PP 38(1988).
29. Reeder, J.R. and Crews J.H.J, "Redesign of the Mixed-Mode Bending Delamination Test to Reduce Nonlinear Effects", *Journal of Composites Technology & Research*, **14**(1), PP 12-19(1992).
30. Tracy, G.D., Feraboli P. and Kedward K.T., "A New Mixed Mode Test for Carbon/Epoxy Composite Systems", *Composites Part A: Applied Science and Manufacturing*, **34**(11), PP 1125-1131(2003).
31. Reeder, J.R. and Crews J.H., "Nonlinear Analysis and Redsign of the Mixed-Mode Bending Delamination Test", National Aeronautics and Space Administration, Langley Research Center: Virginia, PP 42(1991).
32. Kinloch, A.J., "Adhesion and Adhesives", *Science and Technology*, (1987).
33. Jurf, R.A. and Pipes R.B, "Interlaminar Fracture of Composite Materials", *J. Composite Mateials*, **16**, PP 386-394(1982).
34. Arcan, M., Hashin Z. and Voloshin A., "A Method to Produce Plane-Stress States with Applications to Fiber-Reinforced Materials", *Experimental Mechanics*, **18**, PP 141-6(1978).
35. Yoon, S.H. and Hong C.S., "Interlaminar Fracture Toughness of Graphite/Epoxy Composite under Mixed-Mode Deformations", *Experimental Mechanics*, **30**(3), PP 234-239(1990).
36. Ju, S.H. and Rowlands R.E., "Mixed-Mode Thermoelastic Fracture Analysis of Orthtropic Composites", *International Journal of Fracture*, **120**, PP 601-621(2003).
37. Warrior, N.A., Pickett A.K. and Lourenc N.S.F, "Mixed-Mode Delamination - Experimental and Numerical Studies", *Strain*, **39**(4), PP 153-159(2003).
38. Dzenis, Y.A., "Durability and Intelligent Nondestrucrive Evaluation of Adhesive Composite Joints", Ph.D. Thesis, University of Nerbraska-Lincoln: Arlington(1996).
39. Banks-Sills, L., Arcan M. and Bortman Y., "A Mixed Mode Fracture Specimen for Mode Ii Dominant Deformation", *Engineering Fracture Mechanics*, **20**(1), PP 145-157(1984).
40. Miller, K.J. and McDowell D.L., *Mixed-Mode Crack Behavior*, ASTM, PP 333(1999).
41. Rossmanith, H.P. and Miller K.J., "Mixed-Mode Fatigue and Fracture", *1993*, Papers Presented at the International Conference on Mixed-Mode Fracture and Fatigue Held at the Technical University of Vienna, Austria, .
42. Gdoutos, E.E., "Problems of Mixed Mode Crack Propagation", (1984).
43. Sih, G.C. and Theocaris P.S., *Proceedings of the First USA-Greece Symposium on Mixed Mode Crack Propagation*, Sijthoff & Noordhoff, (1980).

44. Gdoutos, E.E., Zacharopoulos D.A., and Meletis E.I., "Mixed-Mode Crack Growth in Anisotropic Media", *Engineering Fracture Mechanics*, **34**(2), PP 337-346(1989).

45. Hou, M., Ye L., and Mai Y.W., "Manufacturing Process and Mehanical Propeties of Thermoplastic Composite Components", *Journal of Materials Processing Technology*, **63**, PP 334-338(1997).

46. Kim, K.-Y. and Ye L., "Interlaminar Fracture Toughness of Cf/Pei Composites at Elevated Temperatures: Roles of Matrix Toughness and Fibre/Matrix Adhesion", *Composites Part A: Applied Science and Manufacturing*, **35**(4), PP 477-487(2004).

47. N. Choupani, Ye L., and Mai Y.-W., "Mixed-Mode Fracture of Adhesively Bonded Joints", Ph.D. Thesis, The University of Sydney(2005).

48. Kohli, D.K., "Improved 121 C Curing Epoxy Film Adhesive for Composite Bonding and Repair Applications: Fm300-2 Adhesive System", *International Journal of Adhesion & Adhesives*, **19**, PP 231-142(1999).

49. Mayhew, R.T. and Kohli D.K., "Development of High Temperature Service Polyimide Based Adhesives for Titanium and Composite Bonding Applications", International SAMPE Symposium and Exhibition (Proceedings) Proceedings of the 1996 41st International SAMPE Symposium and Exhibition. Part 2, **41**(2), PP 1026-1034(1996).

50. D2651-90, A.S., "Standard Guide for Preparation of Metal Surfaces for Adhesive Bonding", (1995).

51. Daghyani, H.R., Ye L., and Mai Y.-W., "Mixed-Mode Fracture of Adhesively Bonded Cf/Epoxy Composite Joints", *Journal of Composite Materials*, **30**(11), PP 1248-1265(1996).

52. Habbit, Karlsson, and Sorensen, "ABAQUS User's Manual Version 6.2.4", (2001).